Supplementary Information for

LILRB4-targeting antibody–drug conjugates for the treatment of acute myeloid leukemia

Yasuaki Anami[a,†], Mi Deng[b,†], Xun Gui[a,†], Aiko Yamaguchi[a], Chisato M. Yamazaki[a], Ningyan Zhang[a], Cheng Cheng Zhang[b,*], Zhiqiang An[a,*], and Kyoji Tsuchikama[a,*]

Author Affiliation
[a] Texas Therapeutics Institute, The Brown Foundation Institute of Molecular Medicine, The University of Texas Health Science Center at Houston, 1881 East Road, Houston, TX 77054
[b] Departments of Physiology and Developmental Biology, The University of Texas Southwestern Medical Center, 6001 Forest Park Road, Dallas, TX 75390
[†] These authors contributed equally.

Corresponding Authors
Cheng Cheng Zhang (Alec.Zhang@UTSouthwestern.edu), Zhiqiang An (Zhiqiang.An@uth.tmc.edu), Kyoji Tsuchikama (Kyoji.Tsuchikama@uth.tmc.edu)

This PDF file includes:

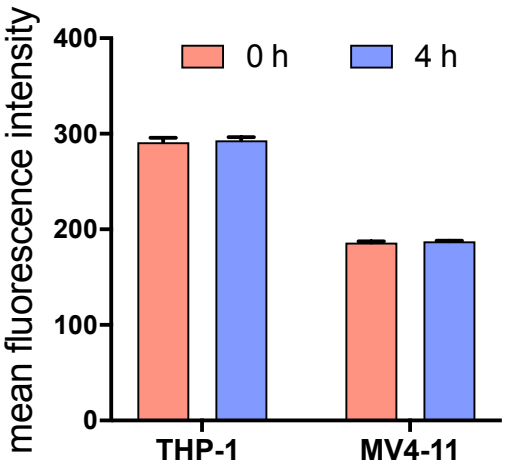

Fig. S1. Expression of LILRB4 on the cell surface is consistent over time. Cells were treated with PBS at 4 °C for 4 h and surface LILRB4 was quantified by FACS. All assays were performed in duplicate. Error bars represent mean ± SEM.

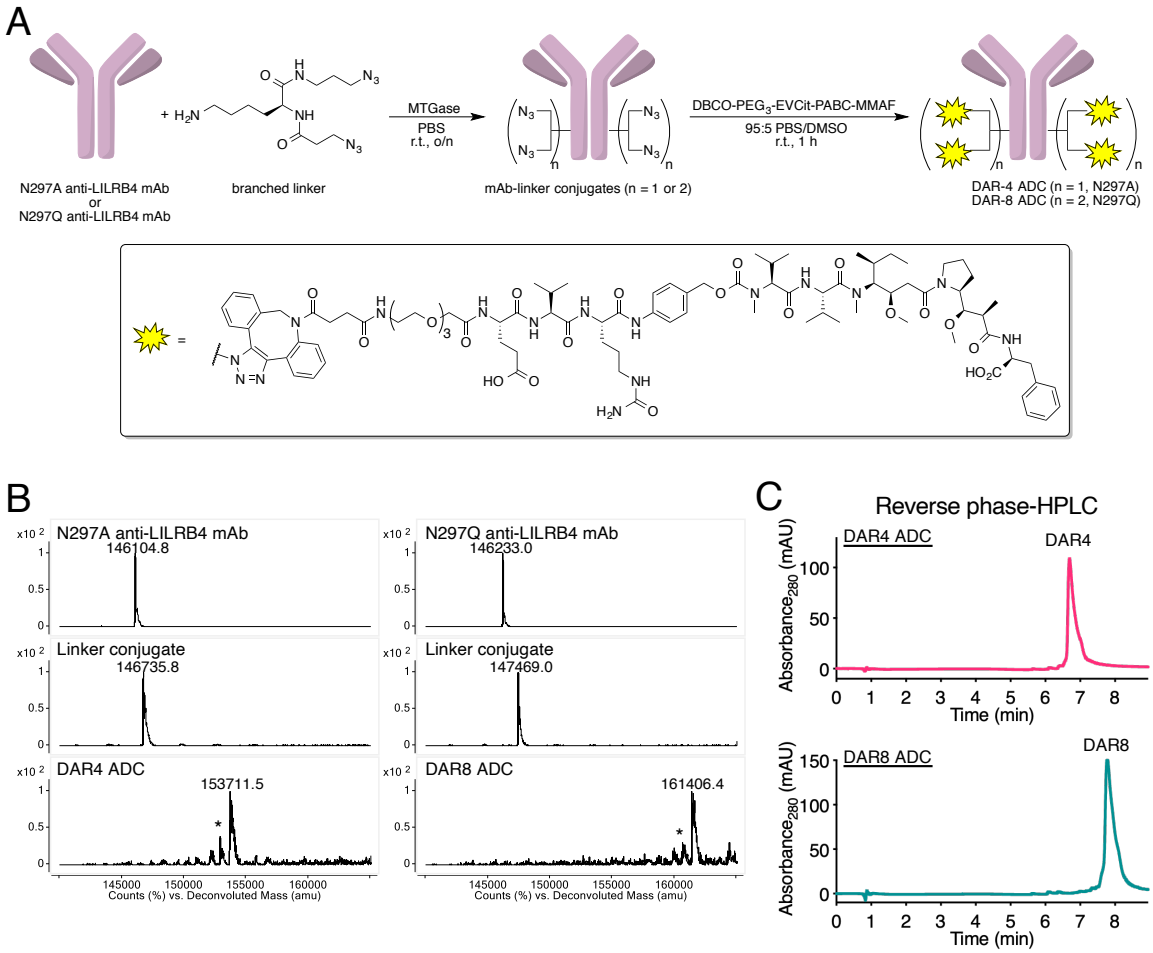

Fig. S2. Construction and characterization of homogeneous anti-LILRB4 DAR-4 and DAR-8 ADCs. (**A**) Stepwise construction of DAR-4 and DAR-8 ADCs by installation of diazide branched linkers using MTGase and following strain-promoted azide–alkyne cycloaddition (yellow spark: DBCO–PEG_3–EVCit–PABC–MMAF module). The chemical structure of the payload module is shown in a box. (**B**) Deconvoluted ESI-mass spectra. Top panel: N297A or N297Q anti-LILRB4 mAb. Second panel: antibody–branched linker conjugate. Third panel: highly homogeneous DAR-4 and DAR-8 ADCs. Asterisk (*) indicates a fragment ion detected in ESI-MS analysis. (**C**) Reverse-phase HPLC traces (UV: 280 nm) of DAR-4 and DAR-8 ADCs before SEC purification.

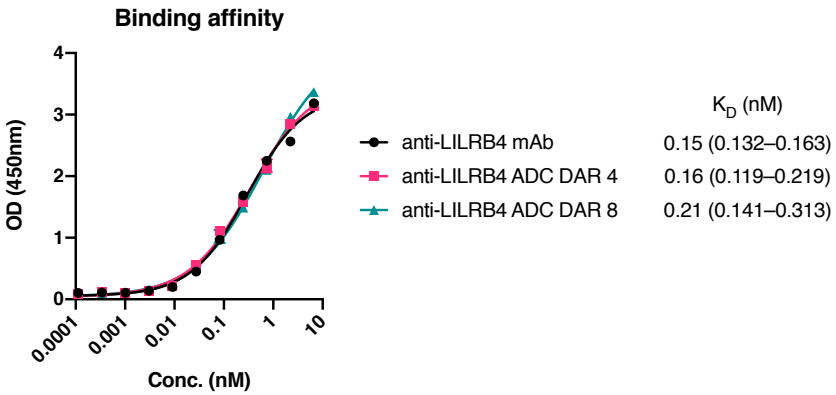

Fig. S3. ELISA binding assay using a recombinant human LILRB4. The binding affinities of unmodified anti-LILRB4 mAb (black), DAR-4 ADC (magenta), and DAR-8 ADC (green) were measured. All assays were performed in duplicate. Error bars represent SEM and values in parentheses are 95% confidential intervals.

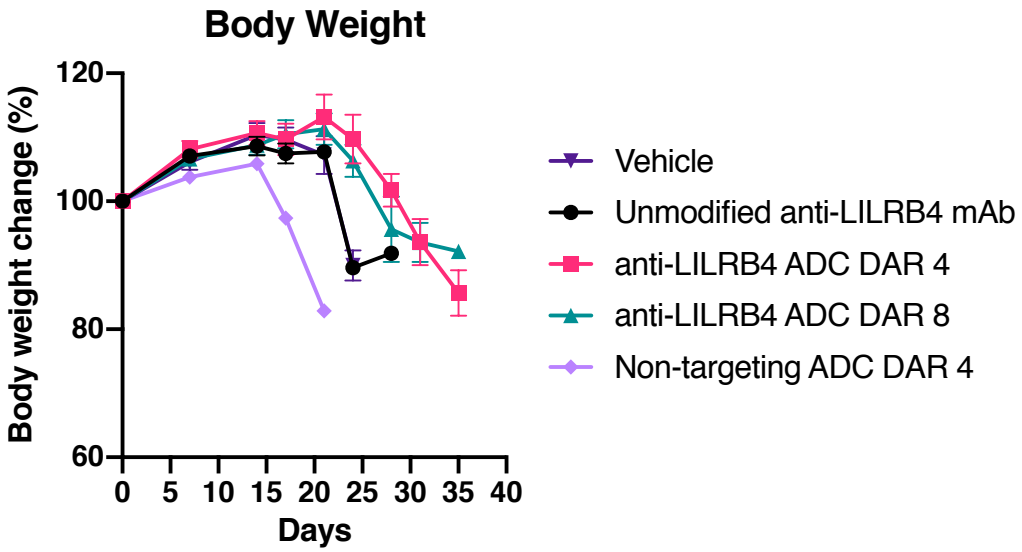

Fig. S4. Body weight change during treatment. Female NSG mice (n = 5) were injected intravenously with THP-1 (1 x 10^6 cells) on Day 0 and treated with each drug (3 mg/kg) or vehicle control (purple) on Day 7, 14, and 21. No significant body weight loss caused by either ADC was observed over the course of study. Error bars represent SEM.

Table S1. EC_{50} values of ADCs in AML cell lines (n = 3). Calculated based on Fig. 3A. Values in parentheses are 95% confidential intervals.

	EC_{50} (nM)		
	THP-1	MV4-11	U937
anti-LILRB4 mAb	–	–	–
anti-LILRB4 ADC DAR4	0.025 (0.0212 – 0.0283)	0.374 (0.2432 – 0.6414)	–
anti-LILRB4 ADC DAR8	0.0093 (0.0077 – 0.0109)	0.0197 (ND – 0.0239)	–
Non-targeting ADC DAR4	–	–	–
MMAF alone	31.08 (27.21 – 35.81)	~168.6	27.01 (23.02 – 32.61)

Table S2. AUC of each conjugate (n = 5). Calculated based on Fig. 4A. Values in parentheses are 95% confidential intervals. AUC, area under the curve.

	$AUC_{total\ mAb}$ (μg day mL^{-1})
anti-LILRB4 mAb	3136 (2961 – 3312)
anti-LILRB4 ADC DAR 4	2629 (2515 – 2742)
anti-LILRB4 ADC DAR 8	645 (604 – 685)

Table S3. Summary of statistical significance.

Main Figures	Method	Asterisk	Comparison	*P* value
Fig. 3B	Welch's *t* test	*	hCB: anti-LILRB4 ADC DAR 4 vs hCB: anti-LILRB4 ADC DAR 4	*P* = 0.0166
Fig. 4A	Welch's *t* test	****	anti-LILRB4 ADC DAR 4 at Day 14 vs anti-LILRB4 ADC DAR 4 at Day 14	*P* < 0.0001
Fig. 4B	Log-rank (Mantel-Cox)	ns	Vehicle vs anti-LILRB4 mAb	*P* = 0.3685
		***	Vehicle vs DAR-4 ADC	*P* = 0.0025
		**	Vehicle vs DAR-8 ADC	*P* = 0.0079

The *P* values correspond to the asterisks in each figure panel; **P* < 0.05; ***P* < 0.01; ****P* < 0.005; *****P* < 0.0001.